Nano Research

ISSN 1998-0124 CN 11-5974/O4
https://doi.org/10.26599/NR.2026.94909262

Research Article

Balancing surface area and electrical conductivity in carbon nanotube composite networks to enhance thermophilic microbial fuel cell performance

Minfang Zhang[1](✉), Mei Yang[1], Ying Zhou[1], Don N. Futaba[1](✉), Masaki Umetsu[2], Chika Tada[3]

[1] Nanocarbon Material Research Institute, National Institute of Advanced Industrial Science and Technology (AIST), 1-1-1 Higashi, Tsukuba, Japan

[2] Graduate School of Environmental Studies, Tohoku University, Aoba-ku, Sendai, Japan

[3] Graduate School of Agricultural Science, Tohoku University, 232-3 Yomogida, Naruko-onsen, Osaki, Miyagi, Japan

Nano Res., **Just Accepted Manuscript** • https://doi.org/10.26599/NR.2026.94909262

https://www.sciopen.com/journal/1998-0124 on Oct. 13, 2026

© The Authors(s)

Just Accepted

This is a "Just Accepted" manuscript, which has been examined by the peer-review process and has been accepted for publication. A "Just Accepted" manuscript is published online shortly after its acceptance,which is prior to technical editing and formatting and author proofing. Tsinghua University Press (TUP) provides "Just Accepted" as an optional and free service which allows authors to make their results available to the research community as soon as possible after acceptance. After a manuscript has been technically edited and formatted, and the page proofs have been corrected, it will be removed from the "Just Accepted" web site and published officially with volume and article number (e.g., *Nano Research*, **2025**, *18*, 94906990). Please note that technical editing may introduce minor changes to the manuscript text and/or graphics which may affect the content, and all legal disclaimers that apply to the journal pertain. In no event shall TUP be held responsible for errors or consequences arising from the use of any information contained in these "Just Accepted" manuscripts. To cite this anuscript please use its Digital Object Identifier (DOI®),which is identical for all formats of publication.

Research Article

Balancing surface area and electrical conductivity in carbon nanotube composite networks to enhance thermophilic microbial fuel cell performance

Minfang Zhang[1]*, Mei Yang[1], Ying Zhou[1], Don N. Futaba[1*], Masaki Umetsu[2], Chika Tada[3]

[1] Nanocarbon Material Research Institute, National Institute of Advanced Industrial Science and Technology (AIST), 1-1-1 Higashi, Tsukuba, Japan

[2] Graduate School of Environmental Studies, Tohoku University, Aoba-ku, Sendai, Japan

[3] Graduate School of Agricultural Science, Tohoku University, 232-3 Yomogida, Naruko-onsen, Osaki, Miyagi, Japan

Received: 6 July 2026; **Revised:** 1 September 2026; **Accepted:** 24 July 2026

Address correspondence to zhanghuanxia818@163.com

Cite this article: *Nano Research*, 2026, 19, 94909262 https://doi.org/10.26599/NR.2026.94909262

Just Accepted

Abstract

Microbial fuel cells (MFCs) enable simultaneous energy generation and organic waste treatment; however, their performance is often limited by inefficient electron transfer at the microbe–electrode interface. Carbon nanotubes (CNTs) have been widely investigated as anode materials owing to their high electrical conductivity and large specific surface area, yet how surface area and electrical conductivity jointly influence anode performance under thermophilic conditions remain unclear. In this study, two types of single-walled CNTs, super-growth CNTs (SG-CNTs), which possess high surface area, and enhanced direct injection pyrolytic synthesis CNTs (eDIPS-CNTs), which possess high electrical conductivity, were used to fabricate anodes individually and in controlled mixtures on stainless-steel mesh substrates. The anodes were evaluated in thermophilic MFCs inoculated with compost-derived microbial communities at 55 °C. All CNT-based anodes exhibited enhanced redox activity relative to CNT-free controls, with distinct redox features observed at −0.55 to −0.60 V vs Ag/AgCl. Notably, the SG-CNT/eDIPS-CNT anode prepared at a 1:1 (w/w) ratio delivered the highest current response and achieved approximately one order of magnitude higher relative electrical output than the CNT-free control. Gas evolution and

microbial community analyses further suggest that CNT composition influences anaerobic microbial electron utilization without markedly inhibiting microbial activity. These findings highlight the importance of the nanoscale CNT-network architecture in optimizing electron transfer in thermophilic MFCs.

Keywords: carbon nanotubes, composite electrodes, electron transfer, thermophilic conditions, bioelectrochemical interfaces, microbial fuel cells.

Just Accepted

1. Introduction

Microbial fuel cells (MFCs) represent a class of bioelectrochemical systems that enable sustainable energy recovery through the direct conversion of organic substrates into electrical energy by electroactive microorganisms [1-3]. In MFCs, microorganisms oxidize organic matter at the anode and transfer electrons to an external circuit either directly, via membrane-bound redox proteins or conductive appendages, or indirectly through soluble redox mediators. Owing to these characteristics, MFCs have been explored for applications including wastewater treatment, waste-to-energy conversion, and decentralized power generation [4-7]. Despite extensive research efforts, the practical implementation of MFCs remains constrained by relatively low power densities and inefficient electron transfer at the microbe–electrode interface [8]. Thus, the anode material plays a central role in governing MFC performance, as it directly influences microbial adhesion, biofilm development, and extracellular electron transfer kinetics. Conventional carbon-based anodes, such as graphite plates [9-10], carbon cloth [11], and carbon felt [12], offer good chemical stability and biocompatibility; however, their limited electrochemically effective surface area and moderate electrical conductivity restrict the density of active sites and contribute to internal resistance.

To overcome these limitations, nanostructured carbon materials have been explored as alternative anode materials. Among them, carbon nanotubes (CNTs) are particularly attractive owing to their high electrical conductivity, large specific surface area, and structural robustness. Previous studies have shown that CNT-modified anodes can enhance microbial attachment and facilitate electron transfer, resulting in improved current generation [13-17]. However, most previous studies have treated CNTs primarily as performance-enhancing additives, demonstrating the benefits of CNT incorporation or comparing CNT-based electrodes with conventional carbon materials, rather than examining how differences among CNT materials themselves affect bioelectrode performance. CNTs represent a broad class of materials with substantial

variations in structure, surface chemistry, and physicochemical properties, including length, diameter, defect density, functional groups, specific surface area, electrical conductivity, and dispersibility. These properties can influence MFC performance through potentially competing mechanisms: increased surface area can promote microbial colonization and biofilm activity, whereas high electrical conductivity is beneficial for efficient electron transport from biofilms to current collectors. In addition, while not an intrinsic tradeoff, commercial CNT materials exhibit a trade-off between accessible surface area and electrical conductivity. Consequently, the combined influence of these properties on electrochemical performance remains insufficiently understood.

Most MFC studies to date have focused on mesophilic operation, whereas thermophilic MFCs have received comparatively less attention despite potential advantages such as accelerated reaction kinetics and enhanced degradation of complex organic substrates [18,19]. This complexity makes thermophilic MFCs a useful platform for examining how conductive anode materials influence microbial electron utilization. Under thermophilic anaerobic conditions, compost-derived mixed microbial communities exhibit multiple competing electron-consuming pathways, including anode respiration and methanogenesis. In such systems, the physicochemical properties of conductive anode materials are expected to influence electron utilization by affecting extracellular and interspecies electron transfer processes [20].

In this context, combining CNT materials with complementary properties provides a rational strategy for elucidating how surface area and electrical conductivity jointly govern anode performance. In this study, thermophilic MFCs inoculated with compost-derived microbial communities were used to systematically evaluate single-walled CNT-based anodes composed of super-growth CNTs (SG-CNTs) [21], characterized by large accessible surface area, and enhanced direct injection pyrolytic synthesis CNTs (eDIPS-CNTs) [22], characterized by high intrinsic electrical conductivity. CNT films consisting of SG-CNTs, eDIPS-CNTs, and their mixtures at controlled ratios were fabricated and evaluated.

By integrating electrochemical behavior and MFC performance with complementary gas-evolution and microbial-community analyses, this study demonstrates that balancing CNT surface area and electrical conductivity is a key materials-design parameter for enhancing thermophilic MFC performance. These findings establish a materials-design principle for CNT-based anodes and provide design guidance for rational electrode engineering in thermophilic bioelectrochemical systems.

Just Accepted

2. Materials and Experimental Methods

2.1 Materials

Two types of single-walled carbon nanotubes, SG-CNTs and eDIPS-CNTs, produced by super-growth and enhanced direct injection pyrolytic synthesis chemical vapor deposition methods, respectively, were used. SG-CNTs (ZEONANO SG101) were purchased from ZEON Corporation, and eDIPS-CNTs (EC1.5p) were obtained from Meijo Carbon Corporation. The physical properties of CNTs are summarized in Table 1. Surface area values were obtained from the manufacturers' technical specifications, whereas electrical conductivity values were obtained from relevant literature [23].

To obtain homogeneous CNT dispersions for CNT-film preparation, CNTs were dispersed in bovine serum albumin (BSA) (Fatty Acid Free; Nacalai Tesque) solution (5 mg mL^{-1}) using a homogenizer (Sonics, 750 mW) for approximately 30 min, yielding CNT dispersions with a concentration of ~2 mg mL^{-1}. BSA was selected as the dispersing agent based on the procedure described in ISO 19337:2023.

Table 1. Characteristics of SG-CNTs and eDIPS-CNTs

	Commercial name	Purity	Diameter (nm)	Surface areas (CNT-film) (m^2/g)	Conductivity (CNT-film) (s/cm)
SG-CNTs	SG101	>99%	3-5	1050	22
eDIPS-CNTs	EC-1.5p	>98%	1.5-2.5	420	358

2.2 Microbial incubation

Compost was obtained from the university farm of Tohoku University located at Kawatabi Filed Center (Yomogida, Naruko-onsen, Osaki, Miyagi, Japan). The compost consisted of soil, cow manure, and plant leaves. Approximately 2 g of compost was dispersed in 25 mL incubation medium consisting of phosphate-buffered saline (PBS, Sigma-Aldrich) supplemented with 0.13 g of glucose (Fujifilm Wako) and 0.4 mL of a vitamin mixture based on NBRC Medium 1067 (biotin: 2 mg/L; folic acid: 2 mg/L; pyridoxine-HCl: 10 mg/L; thiamine-HCl: 5 mg/L; riboflavin: 5 mg/L; nicotinic acid: 5 mg/L; Ca-pantothenate: 5 mg/L; p-aminobenzoic acid: 1 mg/L; vitamin B_{12}: 0.01 mg/L). The suspension was purged with nitrogen gas for about 2 min and immediately sealed with a butyl rubber stopper to establish anaerobic conditions. Anaerobic incubation was carried out at 55 °C with continuous shaking.

To evaluate the effects of CNTs on microbial growth and activity, approximately 5 mL of either BSA solution (control), SG-CNTs/BSA dispersion, or eDIPS-CNTs/BSA dispersion was added to the compost suspension. The mixtures were purged with nitrogen gas for about 2 min, sealed immediately, and incubated at 55 °C for

Just Accepted

approximately 21 days with continuous shaking. All experiments were performed in triplicate.

Gas produced from each compost suspension was collected on days 4, 7, 14, and 21 and quantified. The compositions of the collected gas were analyzed using a gas chromatograph (Shimadzu, GC-14B), where the gases of H_2 , CH_4 , CO_2 , and N_2 were quantified as a function of time.

2.3 Microbial Community Analysis

To evaluate the effects of CNTs on microbial community composition, the microbial incubation was extended to approximately 90 days. After incubation, the entire suspension was stored at −20 °C and subsequently freeze-dried.

Microbial genomic DNA was extracted from each sample using a DNeasy PowerSoil Pro Kit (QIAGEN) according to the manufacturer's protocol. Bacterial and archaeal community structures were analyzed by 16S rRNA gene sequencing (details provided in the supporting information).

2.4 Preparation and structural characterization of CNT Electrode

CNT electrodes were prepared by vacuum filtration of approximately 3 mL of SG-CNT/BSA and eDIPS-CNT/BSA mixed dispersions with several mass ratios (SG/eDIPS=1:0, 9:1, 2:1, 1:1, 1:2, 1:9, and 0:1) onto stainless-steel mesh (60 mesh, SUS 304, plain weave, Tantore Co., Ltd) to form CNT films. The coated meshes were rinsed with ultrapure water and dried at room temperature for approximately 2 days, yielding CNT-film/mesh electrodes. The CNT loading was approximately 4 mg per electrode. Surface morphologies of the CNT electrodes were observed by scanning electron microscopy (SEM) (Hitachi, FE-SEM S-4800) at an acceleration voltage of 5 kV. TEM measurements of the original SG-CNTs and eDIPS-CNTs were performed using a JEM 2010 microscope (JEOL HIGHTECH Co., Ltd.) equipped with a Gatan CCD camera (US1000) operated at 180 kV and 35 μA. For sample preparation, one drop of CNT dispersion was deposited onto a TEM grid, spread evenly, and dried at room temperature.

To evaluate the properties of CNT films prepared with different SG/eDIPS ratios, films were fabricated from the same dispersion volumes without stainless-steel mesh and dried at 120 °C for 30 min. Surface resistance was measured by a resistivity meter (Nittoseiko Analytech, MCP T610) using a four-probe method, and the specific surface area was measured using N_2 gas adsorption-desorption isotherms using the Brunauer-Emmett-Teller (BET) formulation (MicrotracBEL BELSORP_mini). Raman

Just Accepted

spectroscopy was measured using a microRaman spectrometer (inVia, Renishaw, UK) with a 532 nm excitation wavelength. Raman spectra were acquired using six different spots, and the intensity ratios of the G- and D-bands were calculated as the average of these six measurements to evaluate the structural changes associated with mixing at different ratios.

2.5 Electrochemical measurements and MFC evaluation

2.5.1 Cyclic voltammetry

Cyclic voltammetry (CV) measurements were performed using an electrochemical cell (EC Frontier, VB2-S). In this setup, CNT film electrodes were used as the working electrodes, a PEEK-insulated platinum wire served as the counter electrode (EC Frontier, CE-200) and an Ag/AgCl electrode (EC Frontier, RE-T2A) was used as the reference electrode. The electrolyte consisted of compost dispersion obtained after anaerobic incubation at 55 °C for approximately 1 week. The current–potential curves were recorded using a multichannel potentiostat (VMP-300, Biologic) by scanning the potential from −0.2 to −0.8 V versus Ag/AgCl at a scan rate of 5 mV/s.

2.5.2 Evaluation of Microbial Fuel Cell Performance

Microbial fuel cells (MFCs) were assembled using CNT film-coated stainless-steel mesh (2 × 2 cm, ~4 mg CNTs) as the anodes. Carbon felt (2 × 2 cm, ~2 mm thick) was used as the cathode. The anolyte was compost dispersion after anaerobic incubation at 55 °C for approximately 1 week (pH 7.2), while the catholyte was a 50 mM $K_3[Fe(CN)_6]$ solution. The anode and cathode chambers were separated by a proton exchange membrane (Nafion 117, Chemours), and the MFCs were operated at approximately 55 °C. An external resistance of 100 Ω was applied, and the cell voltage was recorded every 20 s over a period of 48 h using a digital multimeter (DMM6500, Keysight, USA).

3. Results and Discussion

3.1 Characteristics of CNT-based electrodes

As summarized in Table 1, both types of SWNTs exhibit high purity. SG-CNTs possess larger diameters and higher specific surface areas, whereas eDIPS-CNTs exhibit higher electrical conductivity. Raman spectra show G-band peaks at ~1592 cm^{-1} and D-band peaks at ~1350 cm^{-1}, with G/D intensity ratios of ~3 for SG-CNTs and ~40 for eDIPS-CNTs, indicating a higher defect density in SG-CNTs and greater crystallinity in eDIPS-CNTs (Figure 1). TEM analysis confirms that eDIPS-CNTs consist of thinner, well-graphitized nanotubes, whereas SG-CNTs exhibit larger diameters and more

Just Accepted

irregular morphologies (Figure 1). Both CNTs were used as purchased without additional surface functionalization. Their FT-IR spectra showed similar features, which suggests that major differences in surface functional groups were not apparent between the two CNT materials (Figure S2, Supporting Information). In BSA dispersions, both CNT types also exhibited similar hydrodynamic sizes of approximately 40 ± 10 nm and zeta potentials of approximately −30 mV.

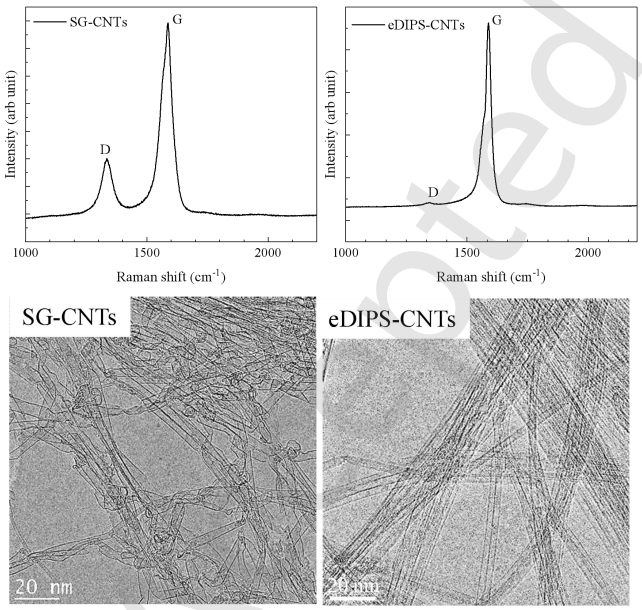


Figure 1. Characteristics of SG-CNTs and eDIPS-CNTs. Raman spectra (top) and TEM images (bottom)

CNT electrodes were prepared by coating stainless-steel mesh with CNT films derived from SG/eDIPS-CNT dispersions at various ratios. SEM images (Figure 2a) show that the film surfaces become smoother and denser with increasing eDIPS content (0–100%). Raman spectra (Figure 2b) show a corresponding increase in the G/D ratio (Figure 2c). The surface resistance of the films decreases with increasing eDIPS content, indicating improved electronic conductivity, with more gradual changes at intermediate SG/eDIPS ratios (Figure 2d). BET specific surface area measurements (Figure 2e) show a monotonic decrease from 270 to 192 $m^2 g^{-1}$ with increasing eDIPS content. These values are lower than those reported for CNT powders in the supplier's catalogue (Table 1), likely because nanotube bundling and packing from homogenous dispersions reduced the accessibility of the nitrogen probe gas molecules to the CNT surface. In addition, partial pore occlusion by residual BSA may also have contributed. Overall,

Just Accepted

these results demonstrate that the properties of the CNT films can be systematically controlled by adjusting the SG/eDIPS ratios.

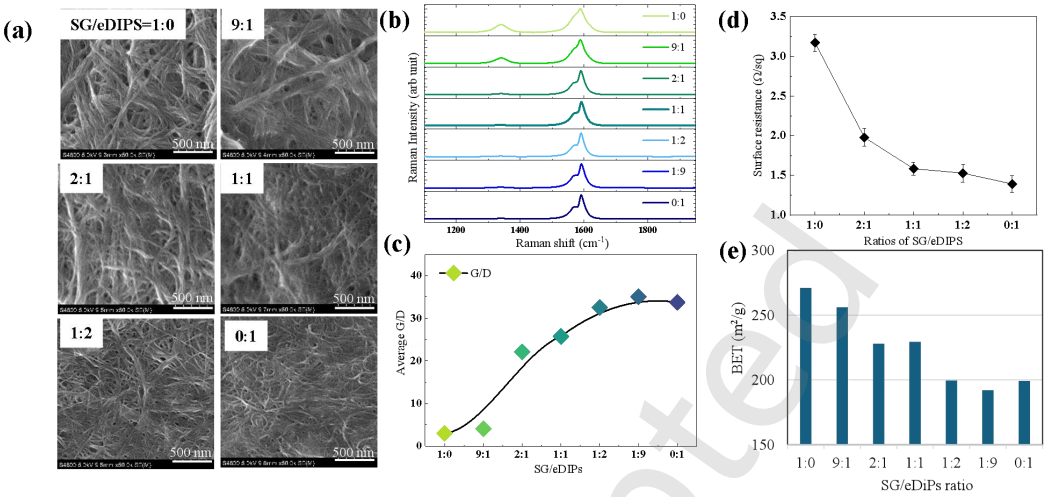


Figure 2. Characteristics of CNT-films used as CNT-based electrodes. (a) SEM images; (b) Raman spectra; (c) Raman G/D band intensity ratios; (d) surface resistance; and (e) BET surface area of CNT films prepared from mixed dispersions of SG-CNTs and eDIPS-CNTs at various ratios (SG/eDIPS = 1:0, 9:1, 2:1, 1:1, 1:2, 1:9 and 0:1).

3.2 Electrochemical behavior of CNT-based anodes

Cyclic voltammetry (CV) was employed to investigate the electrochemical behavior of the CNT-based anodes. A schematic of the voltammetry cell is provided in Figure 3a. Representative CV profiles obtained from the CNT anodes in the compost-derived electrolyte after anaerobic incubation at 55°C for about 1 week are shown in Figure 3b. The current response increased with increasing eDIPS-CNT fraction up to 50% and then decreased with further increase in the eDIPS-CNT content, with the maximum current observed at an SG/eDIPS ratio of 1:1.

Distinct redox peaks at approximately −0.55 to −0.60 V vs Ag/AgCl are observed for all CNT-based electrodes and are likely associated with quinone/hydroquinone redox processes involving humic substances adsorbed on CNT surfaces. The enhanced current observed at an SG/eDIPS ratio of 1:1 suggests that balancing CNT surface characteristics and electrical conductivity influences the electrochemical response of the electrodes.

Just Accepted

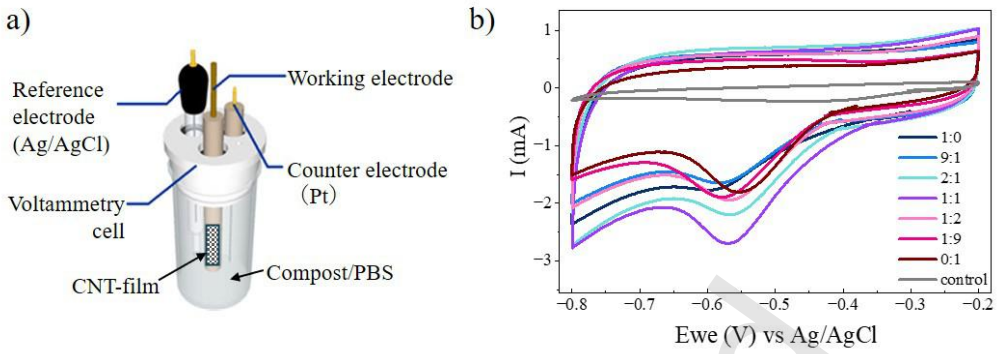


Figure 3. (a) Schematic illustration of the voltammetry cell used for cyclic voltammetry (CV) measurements of CNT-based electrodes. (b) Cyclic voltammograms of CNT-based electrodes prepared from mixed dispersions of SG-CNTs and eDIPS-CNTs at various ratios (SG/eDIPS = 1:0, 9:1, 2:1, 1:1, 1:2, 1:9 and 0:1). The control corresponds to stainless-steel mesh without a CNT film.

3.3 MFC Performance Evaluation

The performance of MFCs assembled with different CNT-based anodes was evaluated at 55 °C by monitoring the cell voltage across a 100 Ω external resistor. A schematic of the MFC configuration is shown in Figure 4a. CNT-film-coated stainless-steel mesh served as the anode, while carbon felt served as the cathode in a ferricyanide catholyte.

The time-dependent voltage profiles (Figure 4b) show that mixed SG/eDIPS-CNT anodes exhibited a rapid increase in voltage during the initial operation period, followed by stable output over 48 hr. This behavior is consistent with microbial acclimation and establishment of effective electron transfer. Among the electrodes tested, mixed CNT anodes, particularly those with intermediate SG/eDIPS ratios, produced the highest and most stable voltage output. In contrast, electrodes composed solely of SG-CNTs or eDIPS-CNTs generated lower voltages, although they remained relatively stable compared with the CNT-free control.

The relative electrical output estimated by integrating the voltage profiles and calculating power using $P=V^2/R$, is shown in Figure 4c. CNT-based anodes produced electrical outputs approximately one order of magnitude higher than the CNT-free control. These results demonstrate that combining SG-CNTs and eDIPS-CNTs enhances MFC performance compared with single-component CNT electrodes.

Just Accepted

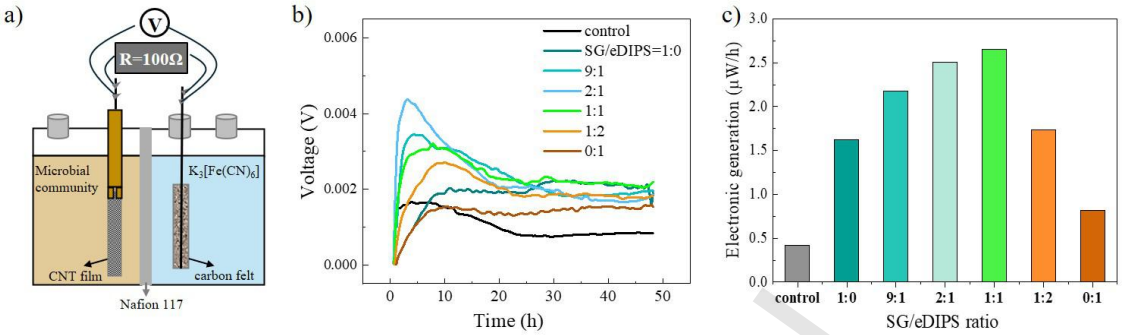


Figure 4. Evaluation of MFC power output using CNT-film electrodes. (a) Schematic illustration of the MFC device used in this study, where CNT-film-coated mesh served as the anode immersed in compost suspension as the anolyte, and carbon felt immersed in $K_3[Fe(CN)_6]$ solution served as the cathode. (b) Voltage profiles measured across an external resistor over 48 h using CNT-film anodes composed of SG-CNTs, eDIPS-CNTs, and their mixtures. (c) Relative electrical output estimated from the integrated voltage profiles in (b) using $P=V^2/R$, where V presents the integrated voltage signal, and R is the external resistance (100 Ω).

3.4 Effects of CNT dispersions on thermophilic microbial communities

To evaluate the influence of CNT materials on thermophilic anaerobic microorganisms, additional incubation experiments were conducted using dispersed CNTs in compost suspensions to analyze gas generation and microbial community composition.

3.4.1 Gas generation

Gas production during anaerobic incubation over 21 days is shown in Figure 5. All samples produced CO_2 and CH_4, indicating active anaerobic metabolism. Compared with the BSA-only control, CNT-containing systems showed slightly increased total gas production (Figure 5a), suggesting a modest enhancement of microbial activity.

Notably, CNT addition, particularly with the more conductive eDIPS-CNTs, resulted in significantly reduced H_2 accumulation together with a slight increase in CH_4 production (Figure 5b). This observation suggests more efficient hydrogen consumption and may indicate enhanced interspecies electron transfer between fermentative bacteria and methanogenic archaea. Together, these results suggest that conductive CNT networks may facilitate interspecies electron exchange under thermophilic anaerobic conditions [24].

Just Accepted

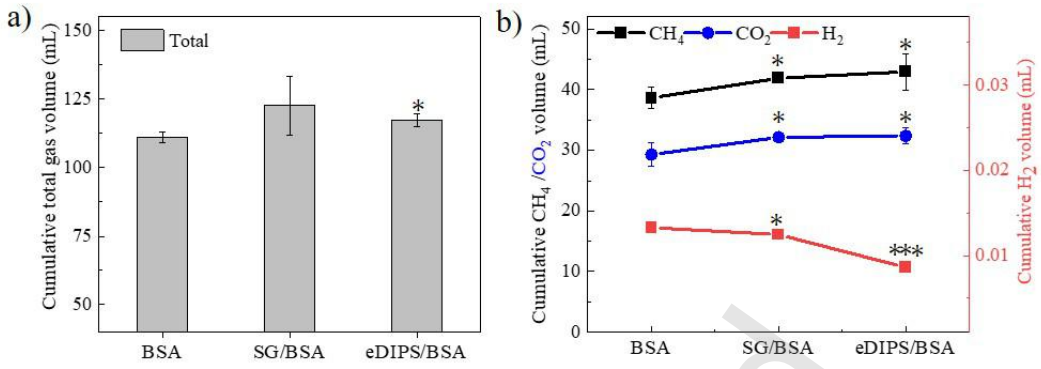


Figure 5. Gas generation from compost suspensions containing BSA, SG-CNT/BSA, or eDIPS-CNT/BSA after anaerobic incubation at 55 °C for approximately 21 days. (a) Cumulative total gas volume. (b) Cumulative volumes of CH_4 , CO_2 , and H_2 determined by GC analysis. The CNT concentration in the dispersions was approximately 0.2 wt%. Statistical significance was evaluated by Student's t-test against the BSA control (*$p < 0.05$, **$p < 0.01$, ***$p < 0.001$).

3.4.2 Microbial Community Analysis

Long-term incubation followed by 16S rRNA gene sequencing and archaeal marker gene sequencing revealed that CNT addition modestly changed microbial community composition compared with the control sample (Figure 6). Both CNT-amended and control systems retained diverse microbial communities, although the relative abundances of several bacterial and archaeal taxa changed in the presence of CNTs. Comparison with the original compost community prior to incubation (Figure S1, Supporting Information) revealed substantial microbial enrichment under thermophilic anaerobic conditions.

In particular, CNT-amended systems showed changes in taxa associated with electroactive or syntrophic microorganisms, alongside shifts in archaeal populations associated with methanogenesis. The observed microbial shifts suggest that CNTs may influence microbial interactions and electron utilization pathways under thermophilic anaerobic conditions. Importantly, however, the overall microbial diversity was maintained. These results suggest that CNTs influence microbial community composition without markedly disrupting the thermophilic anaerobic microbial ecosystem. This indicates limited adverse effects of CNT addition under the present incubation conditions.

Just Accepted

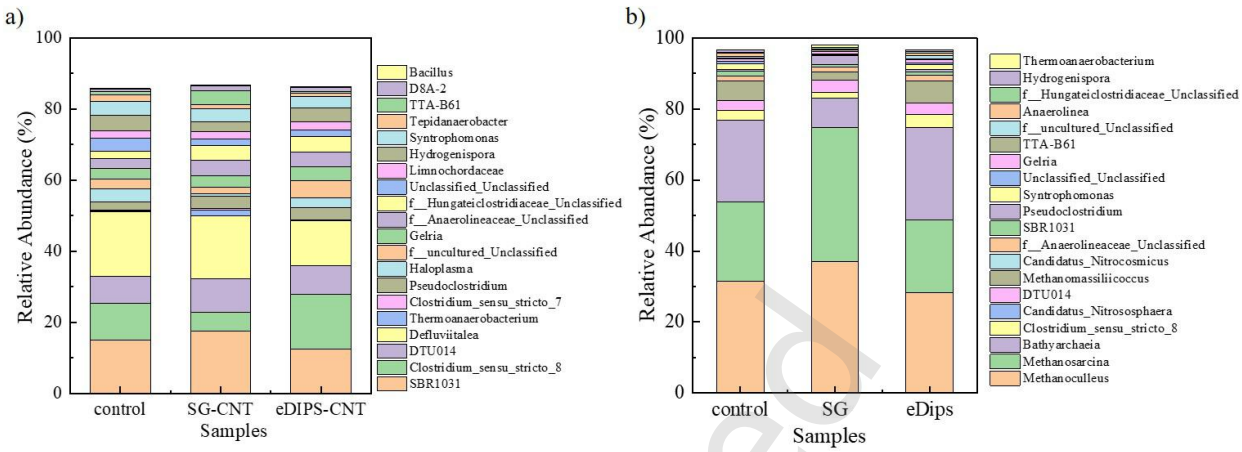


Figure 6. Relative microbial community composition in compost suspensions containing BSA (control), SG-CNT/BSA, or eDIPS-CNT/BSA after anaerobic incubation at 55 °C for 90 days: (a) bacterial communities based on 16S rRNA gene sequencing (top 20 taxa) and (b) archaeal community (top 20 taxa).

3.5 Discussion

This study demonstrates that thermophilic microbial fuel cell performance is governed by the balance between electrode surface area and electrical conductivity. Among the CNT-based anodes investigated, the SG-CNT/eDIPS-CNT composite with a 1:1 mixing ratio consistently exhibited the highest current response and relative electrical output, indicating that neither high surface area nor high conductivity alone is sufficient to maximize bioelectrochemical performance. This optimum likely reflects the need to simultaneously provide accessible microbial interaction sites at the biofilm-electrode interface and continuous conductive pathways for electron transport through the CNT network, thereby facilitating interfacial electron transfer [13-17]. Because both CNTs were used without additional functionalization and showed similar FT-IR features, the observed performance differences are likely dominated by differences in CNT network structure, accessible surface area, and electrical conductivity rather than major differences in surface chemistry.

Electrochemical characterization provides further insight into this behavior. Cyclic voltammetry showed that the 1:1 composite anode exhibited the largest capacitive currents and the most pronounced redox features, suggesting an increased electrochemically active surface area combined with improved electron-transfer pathways. Electrodes enriched in SG-CNTs provide high surface area which expected to be favorable for microbial attachment and adsorption of redox-active compounds

Just Accepted

[11-17]; however, their relatively low intrinsic conductivity may limit charge transport through the electrode network [13, 17]. In contrast, eDIPS-CNT–rich electrodes form highly conductive networks but may reduce the availability of accessible surface area for microbial interactions. At intermediate compositions, the high surface area contributed by the SG-CNTs and the conductive pathways provided by eDIPS-CNTs may be better balanced, which facilitates efficient coupling between microbial electron release and electrode transport processes.

Compared with previous CNT-based MFC studies, which often attribute performance improvements to CNT incorporation in general [13-17], the present work distinguishes the roles of surface area and conductivity by employing two structurally and electrically distinct single-walled CNTs within a unified electrode architecture. As shown in Figure S3 (Supporting Information), increasing the eDIPS-CNT fraction decreased surface resistance but also reduced BET surface area. Consequently, the relative electrical output did not increase continuously with conductivity but reached a maximum at the 1:1 ratio, indicating that both surface area and conductivity contribute to electrode performance. This non-monotonic dependence suggests that the mixed electrode does not simply average the properties of the two CNTs, but instead forms an optimized network architecture at intermediate composition. SEM observations after MFC measurements also showed microbial attachment on all examined CNT-film anodes, with no obvious differences in apparent microbial coverage among the different CNT compositions (Figure S4, Supporting Information). Together, these results highlight the importance of balancing surface area and conductivity in the design of CNT-based bioelectrodes.

Operation under thermophilic anaerobic conditions (55 °C) further emphasizes the robustness and applicability of the CNT composite electrodes. The stable and enhanced performance observed at elevated temperature demonstrates compatibility with thermophilic microbial consortia and suggests that balanced CNT networks can sustain efficient electron transfer under conditions of accelerated metabolic activity and competing electron-utilization pathways, including anode respiration and methanogenesis [18, 19].

Gas production and microbial community analyses indicate that BSA-dispersed CNTs do not adversely affect thermophilic anaerobic microorganisms. Because these experiments were conducted with BSA-dispersed CNTs rather than electrode-bound CNT films, the results should be interpreted as complementary evidence for CNT–microbe interactions rather than direct evidence for the anode mechanism. CNT addition slightly altered microbial activity and microbial community composition while

Just Accepted

maintaining the overall microbial ecosystem. Reduced H_2 accumulation together with slight changes in CH_4 production may reflect more efficient hydrogen consumption and enhanced interspecies electron transfer in the presence of conductive CNT networks [19, 20, 24]. These observations suggest that CNT materials can influence microbial interactions under thermophilic anaerobic conditions.

Overall, this study establishes a materials-design principle for CNT-based bioelectrodes: optimal performance is achieved by balancing accessible surface area with continuous conductive pathways. By integrating electrochemical performance, gas evolution behavior, and microbial community responses, this work provides a framework for the rational design of CNT-based electrodes for efficient energy recovery in thermophilic microbial fuel cells.

4. Conclusion

This study demonstrates that thermophilic microbial fuel cell performance can be significantly enhanced through rational design of CNT-based composite anodes. By combining two types of carbon nanotubes varieties possessing complementary properties (SG-CNTs with high accessible surface area and eDIPS-CNTs with high electrical conductivity), a balanced electrode architecture was achieved that effectively integrated microbial interaction sites with conductive electron-transport pathways.

The optimized 1:1 SG-CNT/eDIPS-CNT anode consistently outperformed single-component and CNT-free electrodes in terms of electrochemical response and relative electrical output under thermophilic conditions. These results demonstrate that optimal performance is achieved not by independently maximizing surface area or conductivity, but by balancing the two properties within a unified electrode architecture.

Complementary gas-production and microbial community analyses further showed that BSA-dispersed CNTs do not adversely affect thermophilic microbial consortia and may influence microbial interactions under anaerobic conditions. Together, these findings establish a materials-design principle for CNT-based bioelectrodes and provide a framework for the rational development of high-performance thermophilic bioelectrochemical systems.

Just Accepted

Reference

[1] Berk, R. S.; Canfield, J. H. Bioelectrochemical energy conversion. *Appl. Microbiol.* **1964**, *12*, 10–12.

[2] Allen, R. M.; Bennetto, H. P. Microbial fuel cells: Electricity production from carbohydrates. *Appl. Biochem. Biotechnol.* **1993**, *39–40*, 27–40.

[3] Logan, B. E.; Hamelers, B.; Rozendal, R.; Schröder, U.; Keller, J.; Freguia, S.; Aelterman, P.; Verstraete, W.; Rabaey, K. Microbial fuel cells: Methodology and technology. *Environ. Sci. Technol.* **2006**, *40*, 5181–5192.

[4] Liu, H.; Ramnarayanan, R.; Logan, B. E. Production of electricity during wastewater treatment using a single chamber microbial fuel cell. *Environ. Sci. Technol.* **2004**, *38*, 2281–2285.

[5] Pandit, S.; Chandrasekhar, K.; Kakarla, R.; Kadier, A.; Jeevitha, V. Basic principles of microbial fuel cell: Technical challenges and economic feasibility. In *Microbial Applications*, Vol. 1; Kalia, V. C., Kumar, P., Eds.; Springer: Cham, Switzerland, 2017; pp. 165–188.

[6] AlSayed, A.; Soliman, M.; Eldyasti, A. Microbial fuel cells for municipal wastewater treatment: From technology fundamentals to full-scale development. *Renew. Sustain. Energy Rev.* **2020**, *134*, 110367.

[7] Malekmohammadi, S.; Mirbagheri, S. A. A review of the operating parameters on the microbial fuel cell for wastewater treatment and electricity generation. *Water Sci. Technol.* **2021**, *84*, 1309–1323.

[8] Choudhury, P.; Uday, U. S. P.; Mahata, N.; Tiwari, O. N.; Ray, R. N.; Bandyopadhyay, T. K.; Bhunia, B. Performance improvement of microbial fuel cells for wastewater treatment along with value addition: A review on past achievements and recent perspectives. *Renew. Sustain. Energy Rev.* **2017**, *79*, 372–389.

[9] ter Heijne, A.; Hamelers, H. V. M.; Saakes, M.; Buisman, C. J. N. Performance of non-porous graphite and titanium-based anodes in microbial fuel cells. *Electrochim. Acta* **2008**, *53*, 5697–5703.

[10] Taskan, E.; Hasar, H. Comprehensive comparison of a new tin-coated copper mesh and a graphite plate electrode as an anode material in microbial fuel cell. *Appl. Biochem. Biotechnol.* **2015**, *175*, 2300–2308.

[11] Liu, J.; Qiao, Y.; Guo, C. X.; Lim, S.; Song, H.; Li, C. M. Graphene/carbon cloth anode for high-performance mediatorless microbial fuel cells. *Bioresour. Technol.* **2012**, *114*, 275–280.

Just Accepted

[12] Hidalgo, D.; Tommasi, T.; Bocchini, S.; Chiolerio, A.; Chiodoni, A.; Mazzarino, I.; Ruggeri, B. Surface modification of commercial carbon felt used as anode for microbial fuel cells. *Energy* **2016**, *99*, 193–201.
[13] Cui, H.-F.; Du, L.; Guo, P.-B.; Zhu, B.; Luong, J. H. T. Controlled modification of carbon nanotubes and polyaniline on macroporous graphite felt for high-performance microbial fuel cell anode. *J. Power Sources* **2015**, *283*, 46–53.
[14] Sun, J.-J.; Zhao, H.-Z.; Yang, Q.-Z.; Song, J.; Xue, A. A novel layer-by-layer self-assembled carbon nanotube-based anode: Preparation, characterization, and application in microbial fuel cell. *Electrochim. Acta* **2010**, *55*, 3041–3047.
[15] Ren, H.; Pyo, S.; Lee, J.-I.; Park, T.-J.; Gittleson, F. S.; Leung, F. C. C.; Kim, J.; Taylor, A. D.; Lee, H.-S.; Chae, J. A high power density miniaturized microbial fuel cell having carbon nanotube anodes. *J. Power Sources* **2015**, *273*, 823–830.
[16] Naveen, P.; Rai, D.; Chauhan, D.; Shahane, S.; Mishra, U.; Bhunia, B. Carbon nanotube based anodes and cathodes for microbial fuel cells. In *Microbial Fuel Cells: Materials and Applications*; Elsevier, 2019; pp. 125–150.
[17] Fan, X.; Zhou, Y.; Jin, X.; Song, R.-B.; Li, Z.; Zhang, Q. Carbon material-based anodes in microbial fuel cells. *Carbon Energy* **2021**, *3*, 449–472.
[18] Carver, S. M.; Vuoriranta, P.; Tuovinen, O. H. A thermophilic microbial fuel cell design. *J. Power Sources* **2011**, *196*, 3757–3760.
[19] Wrighton, K. C.; Agbo, P.; Warnecke, F.; Weber, K. A.; Brodie, E. L.; DeSantis, T. Z.; Hugenholtz, P.; Andersen, G. L.; Coates, J. D. A novel ecological role of the Firmicutes identified in thermophilic microbial fuel cells. *ISME J.* **2008**, *2*, 1146–1156.
[20] Reguera, G. Microbial nanowires and electroactive biofilms. *FEMS Microbiol. Ecol.* **2018**, *94*, fiy086.
[21] Hata, K.; Futaba, D. N.; Mizuno, K.; Namai, T.; Yumura, M.; Iijima, S. Water-assisted highly efficient synthesis of impurity-free single-walled carbon nanotubes. *Science* **2004**, *306*, 1362–1364.
[22] Saito, T.; Ohshima, S.; Okazaki, T.; Ohmori, S.; Yumura, M.; Iijima, S. Selective diameter control of single-walled carbon nanotubes in gas-phase synthesis. *J. Nanosci. Nanotechnol.* **2008**, *8*, 6153–6157.
[23] Shimizu, T.; Kobashi, K.; Nakajima, H.; Muroga, S.; Yamada, T.; Okazaki, T.; Hata, K. Supercapacitor electrodes of blended carbon nanotubes with diverse conductive porous structures enabling high charge/discharge rates. ACS Appl. Energy mater. 2021, 4, 9712-9720.

Just Accepted

[24] Rotaru, A.-E.; Shrestha, P. M.; Liu, F.; Markovaite, B.; Chen, S.; Nevin, K. P.; Lovley, D. R. Direct interspecies electron transfer between *Geobacter metallireducens* and *Methanosarcina barkeri*. *Appl. Environ. Microbiol.* **2014**, *80*, 4599–4605.

Just Accepted

Electronic Supplementary Material

Balancing surface area and electrical conductivity in carbon nanotube composite networks to enhance thermophilic microbial fuel cell performance

Minfang Zhang[1]*, Mei Yang[1], Ying Zhou[1], Don N. Futaba[1*], Masaki Umetsu[2], Chika Tada[3]

[1] Nanocarbon Material Research Institute, National Institute of Advanced Industrial Science and Technology (AIST), 1-1-1 Higashi, Tsukuba, Japan
[2] Graduate School of Environmental Studies, Tohoku University, Aoba-ku, Sendai, Japan
[3] Graduate School of Agricultural Science, Tohoku University, 232-3 Yomogida, Naruko-onsen, Osaki, Miyagi, Japan

Address correspondence to zhanghuanxia818@163.com

Supporting information to https://doi.org/10.26599/NR.2026.94909262

Just Accepted

1. Microbial Community Analysis

1.1. DNA Extraction and Amplicon Sequencing

After approximately 90 days of anaerobic incubation at 55 °C, compost suspensions were collected and freeze-dried prior to microbial analysis. Genomic DNA was extracted using a DNeasy PowerSoil Pro Kit (QIAGEN, Cat. No. 47014) according to the manufacturer's instructions. The original compost prior to incubation was also analyzed for comparison.

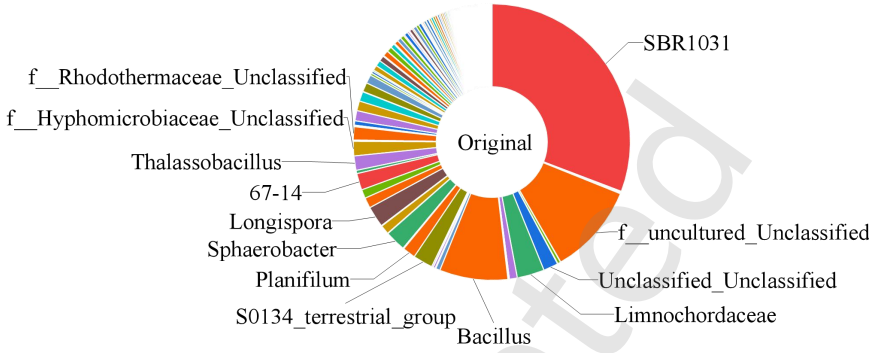
Bacterial community composition was analyzed by 16S rRNA gene amplicon sequencing, and archaeal communities were analyzed using archaeal marker gene sequencing. Amplicon libraries were prepared using universal primer sets targeting the V3–V4 region of the bacterial 16S rRNA gene and archaeal-specific regions. Sequencing was performed on an Illumina platform.

1.2. Sequence Processing and Taxonomic Assignment

Raw sequence data were processed using QIIME2. Quality filtering, denoising, chimera removal, and amplicon sequence variant (ASV) generation were conducted using the DADA2 pipeline. Taxonomic assignment was performed using the SILVA ribosomal RNA database (release 138). Relative abundance analysis was conducted at the genus level.

1.3. Results of Microbial Community Analysis

(a)



(b)

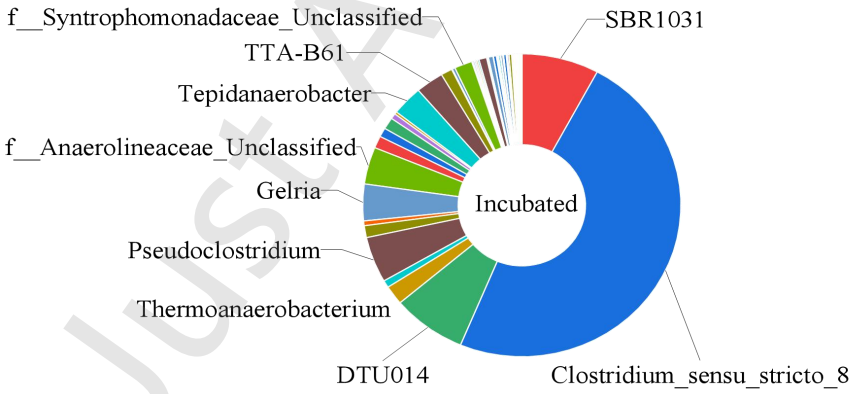


Figure S1. Relative abundance of bacterial communities at the genus level based on 16S rRNA gene sequencing: (a) original compost before incubation and (b) compost after anaerobic incubation at 55 ºC for 90 days in the presence of glucose and vitamins without CNT addition. Taxa with relative abundances greater than 1.5% are labeled.

Just Accepted

2. FT-IR spectra of SG-CNTs and eDIPS-CNTs

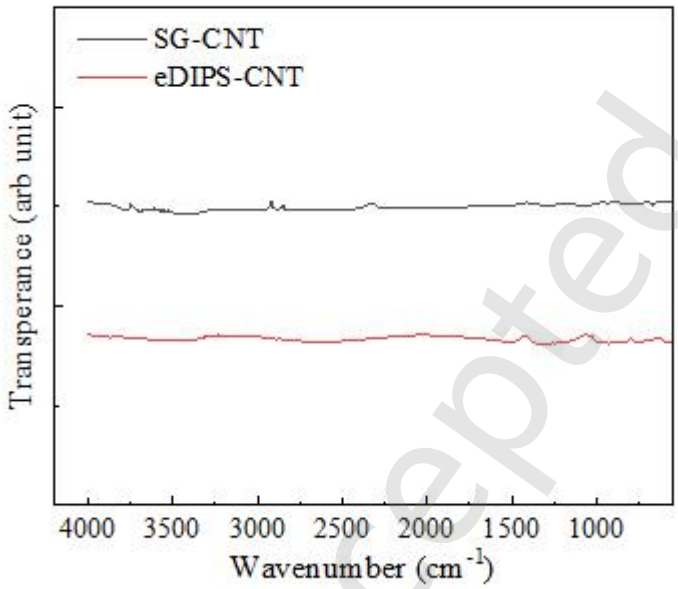
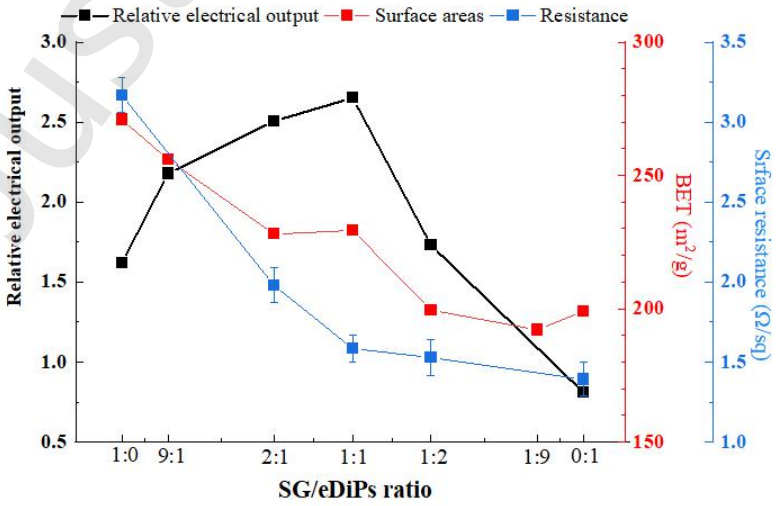


Figure S2. FT-IR spectra of SG-CNTs and eDIPS-CNTs

3. Relationship between CNT-film properties and MFC performance



Just Accepted

Figure S3. Relationship between BET surface area, surface resistance, and relative electrical output.

4. SEM observations of CNT-film anodes after MFC measurements

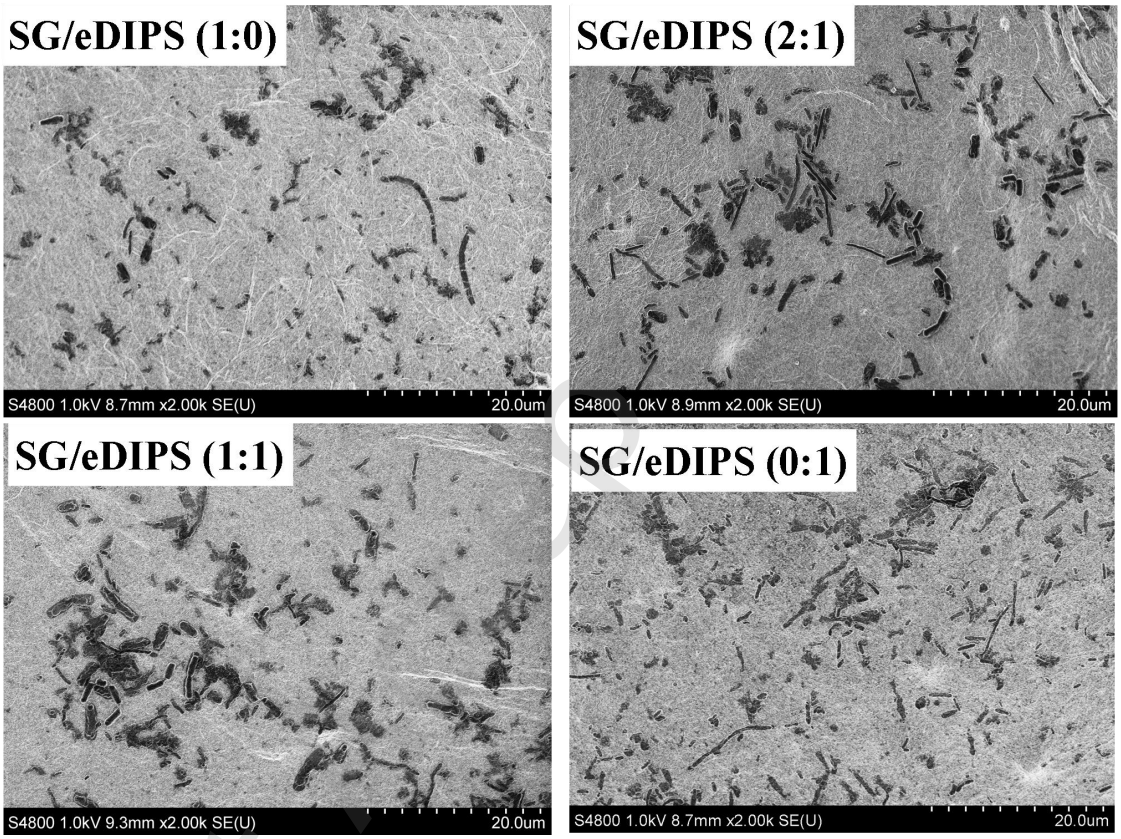


Figure S4. SEM images of CNT-film anodes with different SG-CNT/eDIPS-CNT ratios after MFC measurements.